Int. J. Multiphase Flow Vol. 16, No. 2, pp. 171–185, 1990
Printed in Great Britain.

0301-9322/90 $3.00 + 0.00

AN EXPERIMENTAL STUDY OF THE STABILITY OF LIQUID-FLUIDIZED BEDS

J. M. HAM,[1] S. THOMAS,[2] E. GUAZZELLI,[3] G. M. HOMSY[1] and M.-C. ANSELMET[3]

[1]Department of Chemical Engineering, Stanford University, Stanford, CA 94305, U.S.A.

[2]Department of Chemical Engineering, University of Massachusetts, Amherst, MA 01003, U.S.A.

[3]Department de Physique des Systemes Desordonnes, Université de Provence, Marseille, France

(*Received* 23 *February* 1989; *in revised form* 22 *August* 1989)

Abstract—Experiments are performed to determine if a stable state of uniform fluidization exists for the case of fluidization of small particles by liquids. Such stable states are theoretically possible if the fluidized mixture has a sufficiently large effective elasticity, and stabilization is expected to be more pronounced as the particle size is decreased. Experiments were conducted for a wide range of variables by independently varying particle size, particle density and fluid properties. Careful measurements of the presence or absence of instabilities were made through a combination of flow visualizations and quantitative measurements. We observed stable uniform fluidization over a range of fluid velocities between that required for minimum fluidization, u_{mf}, and that corresponding to the onset of instability waves, u_c. We interpret these experimental results in terms of the recent theory of Batchelor, in which the elasticity is identified with two distinct mechanisms—gradient dispersion and Reynolds stresses due to particle velocity fluctuations. The observed strong dependence of the effective elasticity on the ratio of particle Reynolds number to the fluid/solid density ratio gives support to the conclusion that the main contribution to the elasticity is inertial in origin, and is due to the Reynolds stress due to particle velocity fluctuations.

Key Words: fluidization, instabilities, voidage waves

1. INTRODUCTION

As the flow of fluid upward through an assemblage of particles is increased, the drag force on the particles increases until it is sufficient to balance their buoyant weight. The particles then become free to move and the assemblage, or bed, is said to be fluidized. Below minimum fluidization conditions, the packed bed supports the weight of the particles through contact stresses and the volume fraction of fluid, or void fraction, within the assemblage is nearly independent of flow rate. Above minimum fluidization, the bed maintains the balance between drag and gravity forces by expanding to accommodate the increased flow. In the freely moving state the mixture of fluid and particles displays many of the characteristics of an effective fluid, e.g. the free surface of the bed remains horizontal when the containing vessel is tilted and less-dense objects can be floated in the bed.

Fluidized beds have excellent heat and mass transfer characteristics, which, along with the fact that the fluid–solid mixture can be easily transported in and out of the containing vessel, have led to the use of fluidization in many large-scale processes, such as fluidized catalytic cracking and fluidized coal combustion. Understanding and predicting the behavior of fluidized bed processes is often limited by our understanding of the underlying mechanics of the fluid–solid mixture. For example, instabilities manifest themselves in gas-fluidized beds as "bubbles," i.e. regions in which the fluid is nearly devoid of particles. Bubbles reduce the contact between fluid and particles, limiting the efficiency of the heat and mass transfer. Understanding the origin of these instabilities is an important step in our understanding of fluidized bed mechanics. A comprehensive overview of the science and practice of fluidization can be found in Davidson *et al.* (1985).

To satisfy the need for a fundamental understanding of the mechanics underlying the motion of the two phases, a number of attempts have been made to develop a suitable mathematical theory of fluidization, and of dispersed two-phase flows in general. Two promising approaches to the problem are: (1) to view the solid and fluid phases as interpenetrating continua (hereafter referred to as the continuum approach); and (2) to consider the motion of individual particles in a mean sense (hereafter referred to as the discrete approach). Each of these approaches has advantages and disadvantages and result in final governing equations which are quite similar, a fact which may

allow the two theories to complement each other. Brief descriptions of the continuum and discrete approaches follow; a more complete comparison can be found in Ham (1988).

The continuum approach has at its foundation the assumption that unambiguous local mean properties for each phase can be defined by averaging point properties over a length scale which is large compared to the size of an individual particle in the solid phase, yet small compared to the size of the system. Such an assumption is plausible in concentrated systems such as fluidized beds at or near minimum fluidization. Presuming that local mean properties can be defined, conservation laws governing point quantities, such as mass and momentum, can be averaged to yield continuum balance equations for each phase. Derivation of these continuum equations is discussed by Anderson & Jackson (1967), Drew & Segel (1971a), Homsy *et al.* (1980) and Jackson (1985), among others. The resulting set of continuum equations can be closed only by making additional, constitutive assumptions for the inter- and intraphase forces. Determining the appropriate form for these constitutive equations is the major obstacle in the development of a complete, satisfactory continuum model. Difficulties arise in answering two main questions:

(1) What are the important microscale mechanisms?
(2) How can the effects of the mechanisms be reflected in a continuum framework?

The discrete particle approach need not address the problem of insuring that the microscale is adequately represented in the continuum framework. Instead, governing equations arise directly from ensemble averaging of the equations describing the motion of individual particles in a dispersion. Batchelor (1988) has systematically applied this approach to fluidization and, equivalently, sedimentation. To avoid making untestable hypotheses in the course of developing governing equations, Batchelor restricts his analysis to one-dimensional, unsteady flow. One-dimensional flow, which implies statistical homogeneity on any horizontal plane, allows an equivalence to be made between ensemble means and spatial averages over a horizontal plane. Batchelor proceeds by examining the conservation of particle number and particle momentum in a cylindrical control volume with its axis perpendicular to the uniform horizontal planes. He argues for the existence and nature of various contributions to the momentum balance: flux across boundaries, body forces and interactions of particles within the control volume with other particles and with the fluid. The resulting equations differ from the continuum equations only in their explicit accounting for a net force resulting from hydrodynamic dispersion.

A rigorous discrete approach has the appeal of having no hypotheses which cannot be tested on their own merits, but the current one-dimensional formulation will have limited utility. The one-dimensional theory can be used to investigate nearly homogeneous fluidized beds, but when excursions from homogeneity are large, non-linear effects cause the flow to become two- or three-dimensional, as seen, for example, in the experiments of El-Kaissy & Homsy (1976) and Didwania & Homsy (1981). In order to describe fluidized beds under these conditions, more complete descriptions, allowing three-dimensional motions, are needed. The continuum description can, however, benefit from the existence of the one-dimensional theory, which can provide guidance on the appropriate form for the constitutive models used to close the continuum equations of motion.

The ultimate test of any theory is its ability to describe real systems. The first test is whether a theory admits the correct base-state solution. The commonly-accepted uniform-fluidization base state satisfies the governing equations of both the continuum and discrete approaches. A possible second test is agreement between predictions of linear stability theory and experimental measurements. Linear stability theory applied to both the continuum equations (Anderson & Jackson 1968; Drew & Segel 1971b; Homsy *et al.* 1980 etc.) and the ensemble-average equations (Batchelor 1988) predict that fluidized beds can exhibit growing modes, i.e. they can support, in the form of one-dimensional wave trains, exponential growth of small perturbations to the void fraction, ϵ_0, in a uniform bed. The instability in a fluidized bed requires only the existence of kinematic waves and particle inertia, and results from the phase lag between disturbances in the mean particle velocity and the voidage. However, the uniform base state is not necessarily unconditionally unstable; the bed can be stabilized by what may be considered a bulk elasticity which arises in both approaches. The two approaches differ, however, in the proposed origin, and consequently the expected magnitude, of the bulk elasticity. The continuum description, in its generally accepted

form, has bulk elasticity resulting from direct particle–particle interactions and velocity fluctuations. In the earlier interpretation, this bulk elasticity was not found to be sufficient to prevent instability, and thus fluidized beds were predicted to be unstable at minimum fluidization conditions. The discrete description, on the other hand, has two contributions to the bulk elasticity; one resulting from velocity fluctuations and the other from hydrodynamic dispersion. The magnitude of hydrodynamic dispersion in fluidized beds cannot yet be estimated with any certainty, but considering that $O(1)$ dispersion coefficients have been observed in the sedimentation of dilute and semi-dilute suspensions (Davis & Hassen 1988; Ham & Homsy 1988), Batchelor considered that this contribution to the bulk elasticity may be sufficient to prevent instability. In this context, we should also mention the approach of Foscolo & Gibilaro (1984), who consider the elasticity as arising from an interaction force proportional to the gradient in the volume fraction of particles. Thus, there is predicted to be a gap between minimum fluidization and the onset of an instability when the total contribution to the elasticity of the bed exceeds a certain critical magnitude.

The continuum and discrete descriptions give similar linearized equations for the perturbation void fraction ϵ that we can put in the form of Liu (1982) as

$$A\epsilon_{tt} + B\epsilon_{xt} + (C - Z)\epsilon_{xx} - E(\epsilon_{xxx} + \epsilon_{xxt}) + F\epsilon_t + G\epsilon_x = 0. \quad [1]$$

This resulting linearized equation has been made dimensionless with a characteristic length d, the diameter of the particles, and a characteristic time d/u_0, u_0 being the velocity at the uniform base state. As is well-known, the coefficients A, B etc. are related to the detailed form of the equations and to the expressions used for virtual mass, drag force etc. A detailed discussion is not in order here; rather, we focus our attention on the elastic term $-Z\epsilon_{xx}$ which exists in both descriptions although considered to be of different origins, and to give the criterion for the stability of the fluidized bed.

Equation [1] admits planar wave solutions of the form

$$\epsilon = \epsilon' \exp[ik(x - ct)], \quad [2]$$

where k is real and c is complex. Solutions in which c_i, the imaginary part of c, is positive represent growing disturbances. The uniform base state will therefore only be stable with $c_i \leqslant 0$, $\forall k$. Substitution of [2] into [1] and requiring that $c_i \leqslant 0$, $\forall K$, yields the following criterion for stability:

$$N_m \equiv \frac{\left[A\left(\frac{G}{F}\right) - \frac{1}{2}B\right]^2}{A(Z - C) + \frac{1}{4}B^2} < 1. \quad [3]$$

We can also express this stability criterion in another way and following Liu (1982), we now recast this equation into a form interpretable in terms of wave hierarchies (see Whitham 1974, Chap. 10):

$$\left(\frac{\partial}{\partial t} + a_1\frac{\partial}{\partial x}\right)\epsilon + \tau\left(\frac{\partial}{\partial t} + c_1\frac{\partial}{\partial x}\right)\left(\frac{\partial}{\partial t} + c_2\frac{\partial}{\partial x}\right)\epsilon = v_e\tau\left(\frac{\partial^3\epsilon}{\partial t\,\partial x^2} + \frac{\partial^3\epsilon}{\partial x^3}\right). \quad [4]$$

The waves of different order are clearly displayed by the factored operators. The lower order wave is the familiar kinematic wave found in a sedimenting suspension. The higher order waves are elastic waves. The r.h.s. of the equation is simply a viscous damping term. Stability requires the lower order wave speed, $a_1 = G/F$, to lie between the two higher order wave speeds, c_1 and c_2,

$$c_{1,2} = \frac{B}{2A}\left\{1 \pm \left[1 + \frac{4(Z - C)A}{B^2}\right]^{1/2}\right\}; \quad [5]$$

that is to say, $c_2 < a_1 < c_1$ for stability. The relation between wave speeds and stability is clearer when virtual mass effects associated with the coefficients B and C can be ignored. In this simple case the criterion for stability becomes that the kinematic wave speed, a_1, must be less than an elastic wave speed defined by $(Z/A)^{1/2}$. Clearly, the underlying source of stability is the term associated with the coefficient Z, which can be considered a measure of the elasticity of the bed. The qualitative nature of this result is presented in figure 1, which indicates that stability occurs when Z exceeds some critical value. We also note for future reference that the bed is predicted to first become unstable to long waves, which in an experiment would manifest themselves at very low temporal frequencies.

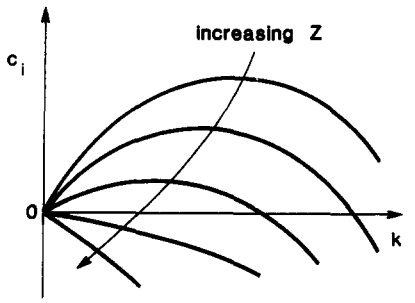

Figure 1. Influence of the elasticity on fluidized bed stability.

The contributions to Z may be considered to be made up of two parts; one arising from the mean square velocity fluctuations in a homogeneous bed and the other due to hydrodynamic dispersion down a concentration gradient:

$$Z = \frac{K_0}{u_0^2} + \frac{\gamma_0(1-R)\hat{D}_0}{\mathrm{Fr}_0}. \qquad [6]$$

Here the subscript 0 implies evaluation at base-state conditions. K_0/u_0^2 is a Reynolds stress associated with particle fluctuations and γ_0 is the mobility. The other quantities appearing are the density ratio,

$$R = \frac{\rho_f}{\rho_s}, \qquad [7]$$

the Froude number,

$$\mathrm{Fr}_0 = \frac{u_0^2}{gd}, \qquad [8]$$

and

$$\hat{D}_0 = \frac{D}{du_0}, \qquad [9]$$

where $\hat{D}_0$ is the dimensionless hydrodynamic (gradient) diffusivity of the particles using a scaling appropriate to Stokes flow (see Davis & Hassen 1988; Ham & Homsy 1988).

We can also define a total dimensionless effective elasticity of the particles as

$$Q = \frac{K_0}{g(1-R)d\gamma_0} + \hat{D}_0. \qquad [10]$$

The criterion of stability can be written as

$$Q > \frac{\mathrm{Fr}}{\gamma_0(1-R)}\{a_1((a_1A - B) + C)\}. \qquad [11]$$

Once expressions are adopted for the various terms, virtual mass coefficient, drag coefficient etc., [11] at the threshold of the instability can be used to determine the magnitude of Q for a given system. We give the details of the explicit working equation we used in the appendix. We emphasize that in experiments, we are unable to discriminate between the two contributions to Q and we therefore measure the total effective elasticity. Only a comparison between the available theories and the observed dependence of Q on the parameters will give information about the relative importance of these terms.

Two careful comparisons between linear stability theory and experimental observations can be found in the literature, those of Anderson & Jackson (1969) and Homsy *et al.* (1980). These studies found general agreement of observations in a liquid-fluidized bed with the predictions of linear stability theory applied to the continuum equations, i.e. the experimentally observed mode for the instability was a one-dimensional axial wave as predicted. These waves apparently appeared at minimum fluidizing conditions. Furthermore, waves were verified to grow exponentially in space.

Homsy *et al.* (1980) also inferred material constants, which are part of the constitutive relations in the continuum description, from measurements of growth rates, phase speeds and wavenumbers, and found them to be "internally consistent and of reasonable magnitude". These studies support the validity of the continuum description, but other experiments call into question its completeness.

Didwania & Homsy (1981) were interested in characterizing the transition, observed by El-Kaissy & Homsy (1976), from linear instability waves to a non-linear, bubbling regime. In the course of their experiments, Didwania & Homsy found a region near minimum fluidization in beds of 0.029 cm glass beads, fluidized with water, in which no instabilities could be detected. Waves were always observed at flow rates just above minimum fluidization for larger particles, and no experiments were performed with particles smaller than these. Didwania & Homsy could not say definitively that a stable liquid-fluidized bed had been observed, since the sensitivity of their detection system was restricted in the experiments with small particles. This was, however, a suggestion that some additional damping mechanism, or additional contribution to the bulk elasticity, may be required for a complete description of fluidization.

We have therefore set as our objectives in this work: (1) to carefully and conclusively determine if stable, uniform fluidization at velocities above minimum fluidization can be attained; (2) to characterize the stable regime; and (3) to compare the experimentally determined characteristics to those predicted by linear stability theory. In section 2, the experimental techniques are described. In section 3, the experimental results are presented. In the first paragraph of this section, we give experimental evidence of a stable region between minimum fluidization and the onset of the planar wave instability. In the second, we deduce from the stability criterion given by Batchelor the total effective elasticity and study its variation with the experimental parameters. Finally, in section 4, the results are discussed and conclusions drawn.

2. EXPERIMENTAL TECHNIQUES AND PROCEDURES

To develop an effective experimental program, we turned for guidance to the experiments of Didwania & Homsy (1981) and the results of linear stability theory, which indicate that, for fixed particle and fluid properties, stability should improve with decreasing particle size. Therefore, our experimental program was as follows. First, we sought to establish the existence or non-existence of a region of stable fluidization characterized by the absence of instability waves at a velocity $u > u_{mf}$ (the subscript mf indicates at minimum fluidization) and void fraction $\epsilon > \epsilon_{mf}$. This was done in a set of preliminary experiments that we will not report here. Second, we sought to measure the gap between (u_{mf}, ϵ_{mf}) and the critical conditions for the onset of instability waves, (u_c, ϵ_c). Finally, we carried out an extensive set of experiments to study the parametric dependence of these quantities on particle size, d, particle density, ρ_p, and fluid viscosity, μ.

2.1. Particle and fluid characteristics

Experiments were done in three separate series in which d, ρ_p and μ were all varied independently. We chose first to fluidize glass beads of fixed density with water, selecting a range of particle sizes which overlapped and ran below that used by Didwania & Homsy (1981). Characteristics of the particles are presented in table 1. Each set was sieved to guarantee that the particles were within adjacent screen sizes, then the set was cleaned with a 33% (vol) HNO_3, 5% HF, 1% Ivory soap solution to remove any surface film. In a second set of experiments, we increased the viscosity μ of the fluid for a given size of particle chosen in the middle of the range (set C), thus determining the dependence of the critical conditions, (u_c, ϵ_c) on μ. In order to vary the viscosity easily, we used a mixture of glycerine and water. Characteristics of the different fluids used are displayed in table 2, and as can be seen, the kinematic viscosity was varied by almost one order of magnitude. Finally, a third set of experiments were performed with different particle densities, for particles in the size range of the first series of experiments, as indicated in table 1.

2.2. Apparatus

A schematic of the apparatus is shown in figure 2. The fluidized bed itself was a cylindrical glass tube of 0.782 ± 0.001 cm i.d. (a bed of 0.779 cm i.d. was used for some of the runs for sets A and B). We constrained our ratios of bed diameter to particle diameter, D_b/d, to fall within a range

Table 1. Particle characteristics

Set	d(cm)	ρ_s(g/cm^3)
A	0.0655 ± 0.0055	2.42 ± 0.007
B	0.0460 ± 0.0040	2.47 ± 0.002
C	0.0325 ± 0.0028	2.49 ± 0.002
D	0.0230 ± 0.0020	2.47 ± 0.001
E	0.0165 ± 0.0015	2.47 ± 0.001
F	0.0325 ± 0.0028	4.14 ± 0.01
G	0.0285 ± 0.0035	1.19 ± 0.01
H	0.0655 ± 0.0025	1.19 ± 0.01

Table 2. Fluid characteristics

Fluid	ν(cS)	A(%, by wt of glycerol)	ρ_f(g/cm^3)
1	1.00	0.00	1.0000
2	1.68	18.30	1.0410
3	2.45	31.96	1.0773
4	4.03	43.80	1.1080
5	8.50	60.02	1.1460

for which wall effects could be neglected while maintaining resolution of the measurement technique, i.e. we worked in the range $10 < D_b/d < 50$. The tube was inspected to insure that its cross section was round and constant along its length. During operation, the tube was securely clamped in position on a rigid support structure, keeping it both straight and vertical.

The flow was distributed uniformly at the bottom of the bed with a special distributor assembly. The distributor assembly consisted of a section of tube filled with 0.0325 cm glass beads, supported at the bottom by a fine mesh screen and packed down at the top by a porous stainless-steel plate. The pores in the plate were small enough to insure a large pressure drop and uniform distribution even at the lowest flow rate used in our experiments. A 1/2″ Swaglock tubing connector at the top of the assembly allowed the porous plate to be sealed between two rubber O-rings and clamped tightly to the bottom of the fluidized bed tube.

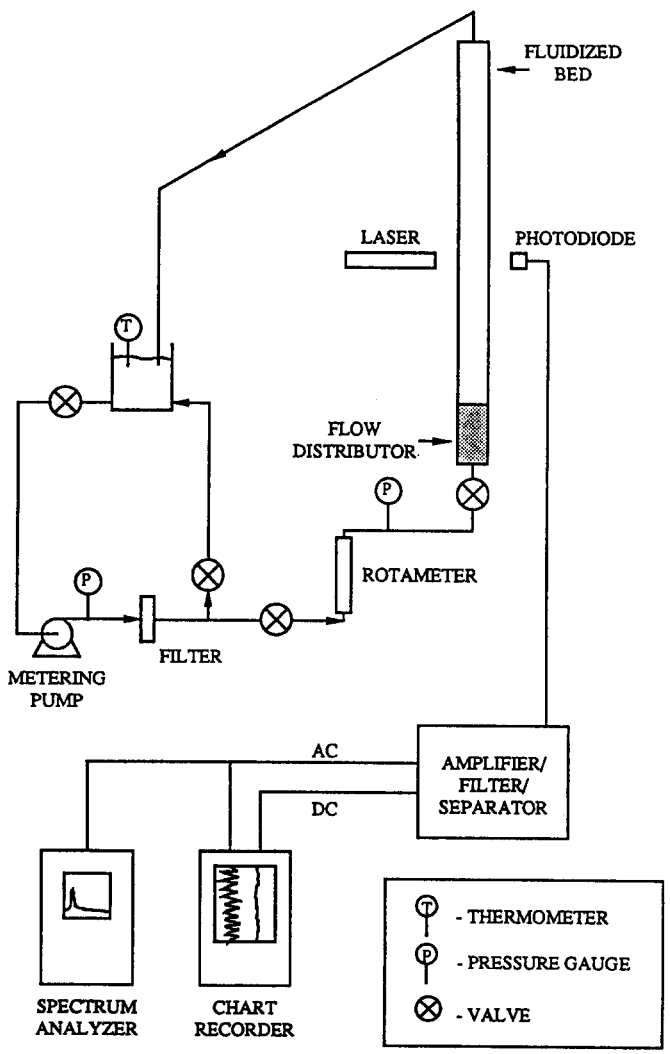

Figure 2. Schematic of the fluidized bed apparatus.

Fluid was circulated through the bed by a piston metering pump (Fluid Metering Inc. model RP-D, 1725 strokes/min), allowing an easy and precise means of flow control. The pump and bed were part of a closed flow loop, containing two different types of flexible tubing: stiff, 1/4″ Teflon tubing and soft, 1/2″ Tygon tubing. The soft tubing connected the pump to the flow loop in order to isolate the fluidized bed from pump vibrations. The soft tubing also collected the overflow and carried it to the reservoir, providing an easy means of diverting the entire overflow into a beaker for gravimetric flow measurement. An in-line filter was placed downstream of the pump to prevent pluggage of the porous plate and a rotameter was included to provide nominal flow rates to aid flow control.

2.3. Optics

The method for detecting instability waves found to be the most appropriate was the light extinction technique originated by Anderson & Jackson (1969), modified by El-Kaissy & Homsy (1976) and used by Didwania & Homsy (1981). The basic principle behind the technique is that the amount of light attenuation by particles in a suspension will be a function of the particle concentration. Fluctuations in the intensity of light transmitted through a fluidized bed can therefore be correlated with fluctuations in the local void fraction. Careful calibration is required to determine the quantitative relation between the magnitude of the intensity and voidage fluctuations, but such calibration was not required for an experiment designed only to detect the onset of coherent fluctuations.

The light-source/detector combination was mounted on an optical rail to keep it accurately aligned and level. The optical rail was attached to the support structure for the fluidized bed and could be moved vertically to position the light at distances above the porous plate ranging from 12 to 120 cm.

Our light source was a 5 mW He–Ne laser (Spectra Physics model 105-2). Our technique did not require the coherence of laser light, but the laser supplied a clean, stable, intense beam of light which could be focused on the photodetector. Localizing the light limited heating of the bed and made temperature control within the flow loop unnecessary. The laser was aligned along a diameter of the bed.

A Hewlett–Packard (model 5082-4220 PIN) photodiode was used to detect the transmitted light. The photodiode was placed at the back of a 12 mm long black plastic tube of 3 mm i.d. The tube was held flush against the side of the bed and aligned opposite the laser, along the same bed diameter. The 3 mm aperture kept our ratios of aperture size to particle diameter roughly in line with those used in the experiments of El-Kaissy & Homsy (1976) and Didwania & Homsy (1981).

2.4. Signal processing

Processing of the intensity signal from the photodiodes consisted of five parts: (1) amplification; (2) filtering; (3) separation of the a.c. and d.c. components; (4) recording of the a.c. and d.c. and (5) spectral analysis of the a.c. The amplifier converted the μA current signal from the photodiode to a voltage signal for further processing, and the filter eliminated fluctuations of frequency greater than approx. 50 Hz, as the signal of interest was anticipated to be in the 0–10 Hz range. The gain on the amplifier could be adjusted from 10^6 to 10^8 V/μA. Separation of a.c. and d.c. was accomplished by extracting the d.c. component from the signal with an active low-pass filter (time constant = 20 s), then substracting the d.c. from the total signal to isolate the a.c. The a.c. was amplified after separation with an amplifier of 100 V/V gain.

The d.c. and a.c. signals were recorded on a two-channel Gould Brush 220 strip chart recorder. The d.c. signal was also monitored with a Fluke model 8600A digital multimeter. The a.c. signal was sent on to a Honeywell/Saicor model SAI-51C real-time spectrum analyzer. The spectra from the analyser were viewed on an oscilloscope and plotted for later evaluation on a Hewlett–Packard 7015B x–y recorder.

2.5. Procedure

The procedure for each particle–fluid set was the same. For most of the experiments, the initial packed bed height was approx. 40 cm. Once the entire charge of particles was in the bed, fluid was circulated through the bed at a flow rate sufficient to expand the bed to the top of the tube. The

bed was operated in this expanded state for more than an hour to release any trapped air bubbles and to clear out any small impurities.

When the start-up procedure was over, the flow rate was lowered until the bed height was approx. 70 cm. The bed was allowed to come to a steady-state and the electronics were allowed to pass through their transients before any measurements were made. Steady-state was verified by observation of a fixed height for the fluidized bed (measured with a cathetometer) and a steady d.c. signal from the photodiodes. At steady-state the flow rate through the bed was measured gravimetrically and the bed height recorded. The a.c. and d.c. signals were recorded during this time, and a spectrum analysis was performed on the a.c. signal. The same measurements were repeated at a sequence of flow rates covering the range between the initial expanded state and a completely packed bed.

The results from a sequence of runs moving down from the expanded state were examined to find both the minimum fluidization point and the critical point, followed by another sequence of runs. The procedure at each step in the repeat sequence was the same as in the original sequence, but the flow rates examined were concentrated around the critical and minimum fluidization points. If the threshold did not coincide with minimum fluidization, then the reversibility of the threshold was examined by moving back and forth through the critical point to observe any hysteresis.

The expansion and stability characteristics for each set were determined in the manner described above, then the entire procedure was repeated a second time. The results from the first and second passes through the experimental program were to be compared to determine the repeatability of the threshold measurements.

3. EXPERIMENTAL RESULTS

In order to be successful in determining if a state of stable fluidization exists, it is necessary to measure two velocities: that for minimum fluidization and that for onset of instabilities. The minimum fluidizing velocity, u_{mf}, was taken to be the velocity at which a bed first begins to expand, and the velocity for onset of instabilities, u_c, was taken to be the velocity for which coherent, wave-like fluctuations could be seen, detected and characterized.

3.1. Experimental evidence of a stable bed

The expansion characteristics may be described by the Richardson–Zaki relation. Typical expansion data are shown in figures 3(a, b) in the base of set C fluidized with water. Figure 3(a)

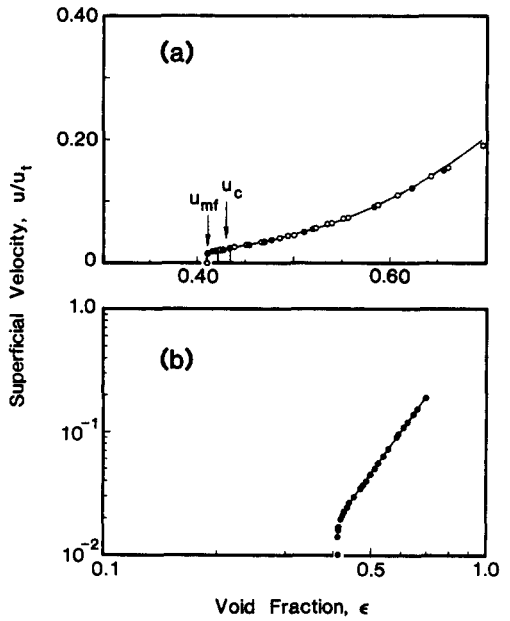

Figure 3. Fluidized bed expansion behavior for particle set C and fluid 1 (water): (a) expansion data on linear coordinates, showing u_{mf} and u_c; (b) data on log coordinates showing the fit to the Richardson–Zaki power law.

Table 3. Fluidized bed expansion characteristics

Set	Fluid	D_d/d	u_t(cm/s)	n	ϵ_{mf}	u_{mf}(cm/s)
A	1	12	10.05	3.47	0.407 ± 0.001	0.4500 ± 0.0500
B	1	17	7.55	3.96	0.409 ± 0.002	0.2200 ± 0.0200
C	1	24	4.97	4.42	0.410 ± 0.020	0.0970 ± 0.0100
D	1	34	3.21	4.47	0.398 ± 0.001	0.0520 ± 0.0060
E	1	47	1.66	4.68	0.411 ± 0.001	0.0260 ± 0.0020
C	2	24	3.87	4.66	0.407 ± 0.001	0.0590 ± 0.0060
C	3	24	2.91	4.82	0.410 ± 0.001	0.0400 ± 0.0040
C	4	24	1.97	4.85	0.409 ± 0.010	0.0260 ± 0.0030
C	5	24	1.04	5.16	0.413 ± 0.010	0.0109 ± 0.0011
F	1	24	9.22	4.22	0.412	0.192
G	1	27	0.82	5.28	0.447	0.010
H	1	12	2.81	4.68	0.443	0.053

shows such data on linear coordinates, while figure 3(b) shows the same data on the more conventional logarithmic coordinates. The value of u_{mf} was taken to be the velocity at which the bed begins to expand, and was measured by identifying the break in the curves of expansion vs velocity. The values measured in this fashion agreed well with those calculated using standard correlations. The data include replicate runs, in which it is seen that the expansion characteristics are repeatable, and do not exhibit substantial hysteresis. The results of least-squares fits to the standard relation, $u = u_t \epsilon^n$ are included in figures 3(a, b). From such data, the exponent, n, as well as the velocity u_{mf} may be measured, and the results from all the cases studied are given in table 3.

The stability characteristics of the bed were determined by visual observation, examination of the strip chart recordings and evaluation of the spectra, with substantial agreement between the three. In the initial expanded fully-fluidized state, the particles displayed large-scale motion, the a.c. signal was noisy and the spectra had many broad, ill-defined peaks. As the flow rate was decreased, the motion became more coherent, finally reaching a state in which planar waves became evident. In the planar wave region, the spectra became dominated by a single peak at a frequency,

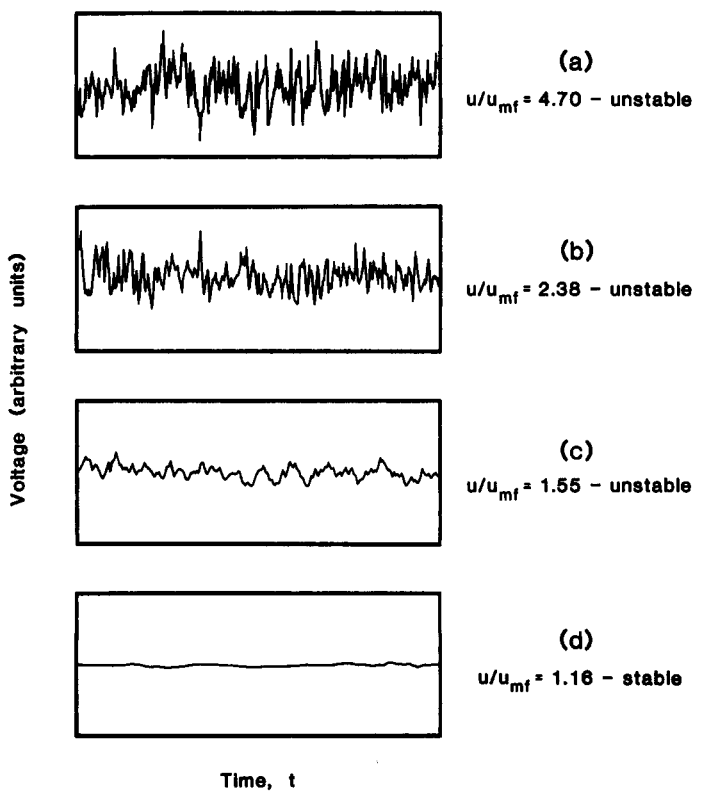

Figure 4. Intensity traces during the crossing from an unstable to a stable fluidized bed.

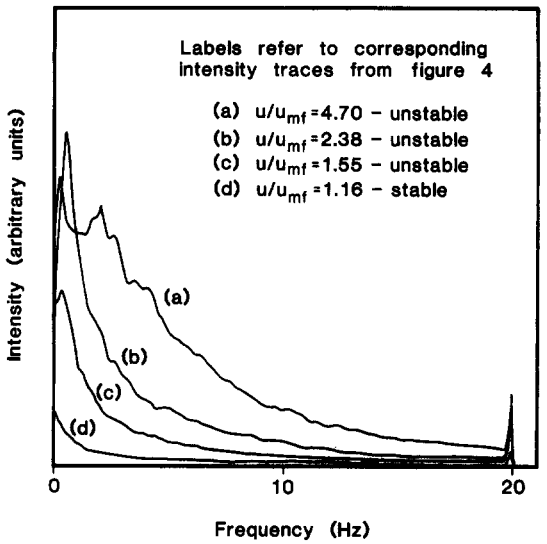

Figure 5. Power spectra crossing from an unstable to a stable fluidized bed.

$f \leqslant 1.5$ Hz. Further decreases in the flow shifted the peak to a lower frequency and diminished the amplitude of the fluctuations in a continuous fashion. Finally, at some point, the peak of the spectra dropped to below 0.1 Hz and coherent fluctuations of the a.c. signal disappeared. We verified that such a condition corresponded to stability by simultaneously monitoring the d.c. component of the signal with time, which also showed no fluctuations. This change in behavior was considered to represent the crossing of the threshold between an unstable and a stable bed. An example of typical traces for set C fluidized by water is presented in figures 4(a–d), with the crossing occurring between figures 4(c) and 4(d). The corresponding spectra are given in figure 5. It should be noted that the frequency of the wave shifted toward zero while approaching the threshold of the instability. This behavior is shown in figure 6, in which the frequency of the coherent wave is plotted against the Froude number (or equivalently, fluid velocity). It is seen that the data, when extrapolated to zero frequency, show a coincidence between the critical velocity measured as described above, and the velocity at which the frequency vanishes. This behavior agrees with the theoretical expectations, noted in the introduction, that the first unstable mode is of low frequency.

Since the wavelength of the instability diverges at the threshold, we were concerned that the finite length of the bed would prevent observation of extremely long waves. These are general considerations in experimental observations of any convective instability near the threshold, where

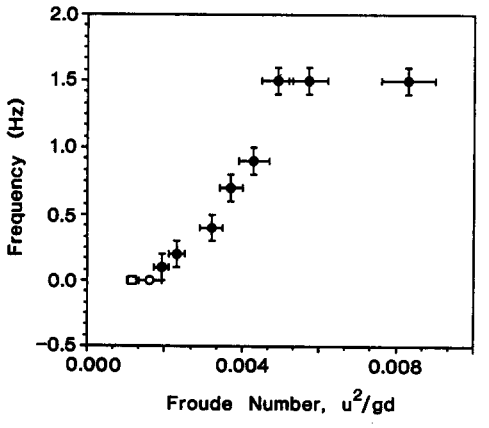

Figure 6. Frequency vs Fr for set F and fluid 1 (water): ○, critical conditions; □, minimum fluidization.

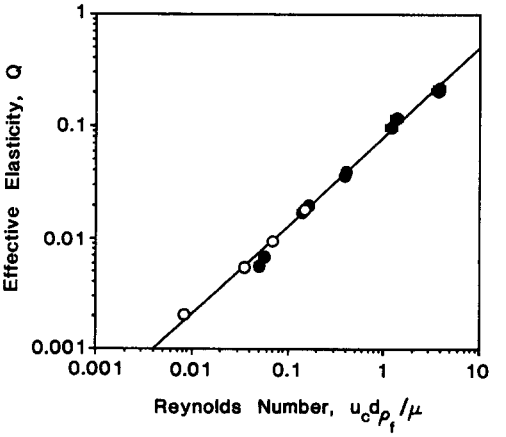

Figure 7. Dependence of Q on particle Re at critical conditions: ●, fluidization with water as the working fluid, variable particle size; ○, fluidization of particle group C with different fluids. The line is the best-fit power law through the data.

Table 4. Fluidized bed stability characteristics

Set	Fluid	ϵ_c	u_c(cm/s)
A	1	0.429 ± 0.005	0.5300 ± 0.0600
B	1	0.425 ± 0.004	0.2500 ± 0.0300
C	1	0.428 ± 0.006	0.1170 ± 0.0140
D	1	0.410 ± 0.003	0.0600 ± 0.0060
E	1	0.439 ± 0.010	0.0350 ± 0.0050
C	2	0.424 ± 0.005	0.0710 ± 0.0080
C	3	0.428 ± 0.003	0.0490 ± 0.0050
C	4	0.448 ± 0.003	0.0400 ± 0.0040
C	5	0.464 ± 0.008	0.0198 ± 0.0025
F	1	0.419 ± 0.007	0.227 ± 0.019
G	1	0.452 ± 0.008	0.012 ± 0.001
H	1	0.462 ± 0.009	0.075 ± 0.006

Table 5. Effective elasticity vs particle Re and density ratio

Set	Fluid	Q	Re_c	R	Re_c/R
A	1	0.206	3.70	0.413	8.96
		0.215	3.77		9.13
		0.215	3.79		9.17
B	1	0.117	1.35	0.405	3.33
		0.098	1.20		2.96
C	1	0.036	0.385	0.402	0.96
		0.039	0.406		1.01
D	1	0.017	0.140	0.405	0.35
		0.196	0.163		0.40
E	1	0.0057	0.050	0.408	0.12
		0.0068	0.057		0.14
C	2	0.0181	0.148	0.418	0.35
C	3	0.0094	0.069	0.433	0.16
C	4	0.0055	0.035	0.445	0.08
C	5	0.002	0.0083	0.586	0.01
F	1	0.0938	0.802	0.242	3.32
G	1	0.0031	0.039	0.839	0.05
H	1	0.0342	0.565	0.843	0.67
H		0.0353	0.557		0.66

growth rates are small, and is particularly important for long-wave instabilities. Accordingly, we repeated one of the experiments (set H with water), with a packed bed of only 20 cm in depth, and observed the same critical velocity, within the errors of the experiment.

An example of the location of the threshold for the particle set C fluidized with water is depicted in figures 3(a, b). The instability points for all other systems were obtained in a similar fashion and the measured values of (u_c, ϵ_c) are presented in table 4. The location of the threshold was found to be the same when approached from $u < u_c$ (expanding bed) as when approached form $u > u_c$ (contracting bed), indicating a non-hysteretic transition between a stable expanded state and the wavy state. Many experiments were repeated, with the same results obtained to within the errors, as indicated in tables 3 and 4.

3.2. Estimation of the effective elasticity

These studies prove conclusively that, with sufficiently small particles, it is possible to obtain a uniformly expanded, stable fluidized bed. The only available theory with which to interpret such observations is one based upon an effective elasticity as the mechanism of stabilization, as described in the introduction and in the appendix. The dimensionless stability parameter in this theory is the dimensionless quantity Q. Experimental values for Q were calculated using the working equation, [A.7] in the appendix, where all the quantities on the r.h.s. of that equation are measured. It is important to emphasize that the specific values of Q depend upon specific relations for the drag curve, virtual mass expressions, mobility etc., that are adopted in the theory. In this sense, we consider the stability data in table 4 to be the important primitive results of the experiments, and the computer values of Q to be derived quantities. Improved theoretical expressions for the coefficients in [11] may allow improved estimates of Q. As we will see, important inferences about the physical mechanisms may be made by examining the dependence of Q on the parameters describing the fluid–particle mixture.

4. DISCUSSION AND CONCLUSIONS

4.1. Variation with particle size and fluid viscosity

We first discuss the results for the first two series of experiments in which both particle size and fluid viscosity were varied. The calculated values of Q are plotted as a function of the particle Reynolds number at critical conditions, Re_c, in figure 7. A number of points may be made regarding these results. The first is that the effective dispersion coefficient scales uniquely with Reynolds number for these two series of data. Recall that for the data in figure 7, particle size, fluid velocity and fluid properties were all varied *independently*. Second, the most surprising aspect of these data is the strong dependence on Re, even for the relatively small Re values involved. The best fit curve through the data indicates that $Q \sim (Re_c)^{0.79}$. Figure 8(a) presents the same data on linear

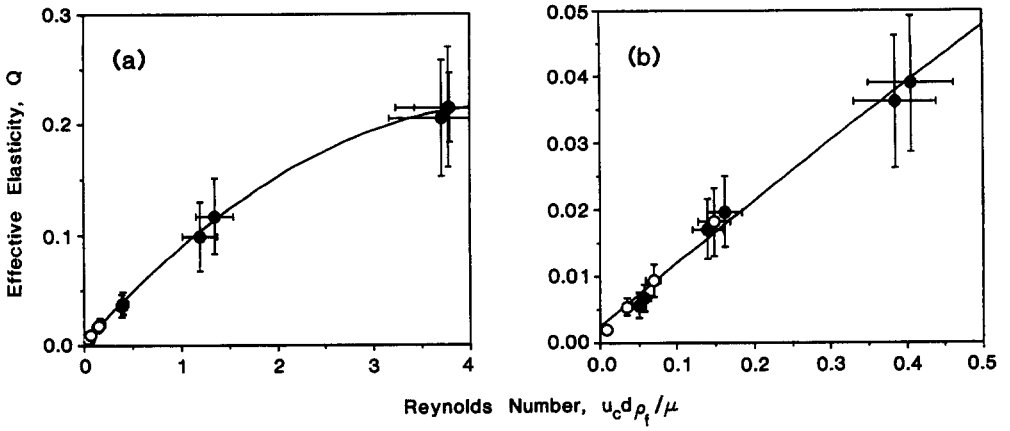

Figure 8. Dependence of Q on particle Re at critical conditions. The solid curve is the best quadratic fit through the data: (a) all data; (b) data for small Re.

coordinates, with a best fit curve indicating that

$$Q = 2.3 \times 10^{-3} + 9.6 \times 10^{-2}\,\mathrm{Re}_c - 1 \times 10^{-2}(\mathrm{Re}_c)^2.$$

Higher order polynomial fits to the data resulted in poorer fits. The strong Re dependence is reflected in the small intercept and the fact that the data are very nearly linear in Re_c for small Re_c, as shown in figure 8(b).

4.2. *Variation with particle density*

A third series of experiments in which the particle *density* was varied leads to important insight as to the mechanism of stabilization. In figure 9, we show values of Q for the three data in this series compared with the general behavior from the first two series. We notice that the datum for the high density particles lies above the best-fit line corresponding to the previous results, while the data for the low density particles falls below. This indicates that the effective elasticity depends not only upon Re, but, as expected from general dimensional analysis, on the ratio R of particle to fluid density. Moreover, the variation, at least over this range of R, is systematic. This suggested that we attempt to find a universal scaling of Q with a combination of Re_c and R, the simplest being Re_c/R. The corresponding plot of Q vs Re_c/R is shown in figure 10. It is seen that *all* the data scale well with this combination of variables, with the best fit,

$$Q = \left(\frac{\mathrm{Re}_c}{R}\right)^{0.77}.$$

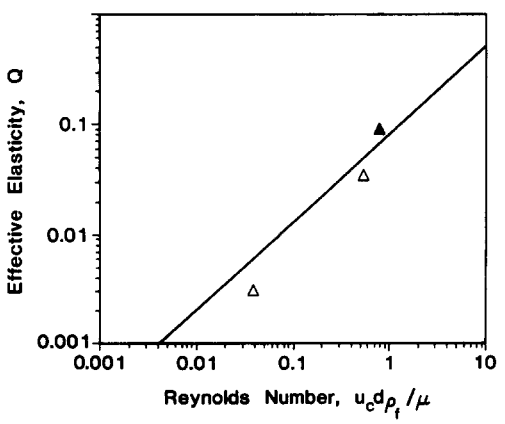

Figure 9. Dependence of Q on particle Re; effect of varying particle density: ▲, fluidization of set F ($\rho_s = 4.14$ g/cm^3) with water; △, fluidization of sets G and H ($\rho_s = 1.19$ g/cm^3) with water; the solid line is the best fit of the data for the first two series of experiments ($\rho_s = 2.47$ g/cm^3).

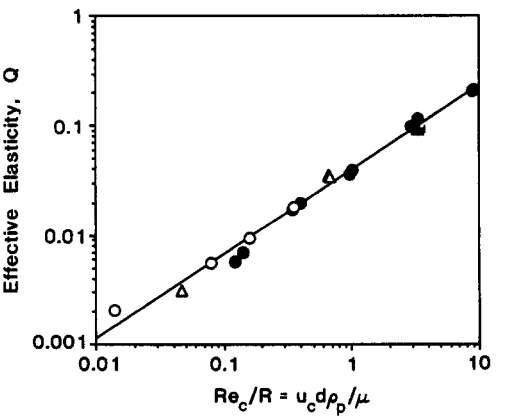

Figure 10. Dependence of Q on Re_c/R. Same notation as in figures 7 and 9.

Our experimental observations are in qualitative agreement with the prediction from linear stability theory that a bulk elasticity can stabilize beds of small particles. We have found that there is a gap between minimum fluidization and the onset of the wavy instability where a stable fluidized state can be obtained. Stable fluidization is a robust phenomenon, with the location of the threshold between the stable and unstable states exhibiting good repeatability and no hysteresis. We have observed that the frequency of the waves decreased to zero when approaching the threshold by decreasing the flow rate. This is in agreement with the fact that the stability criterion [3] guarantees stability to disturbances of all wavelengths.

Interpreting these results in terms of available theory, we have deduced the stability parameter, a dimensionless effective elasticity, Q. We find that Q is not independent of the diameter of the particle or of the viscosity of the fluid. As discussed in the introduction, Q is considered to be made up of two parts, one coming from a Reynolds stress due to particle velocity fluctuations and the other due to hydrodynamic dispersion down a concentration gradient. While the statement made by Batchelor that the one-dimensional theory presented does not contain parameters that cannot be measured independently is correct, those measurements do not presently exist for the particle concentrations of interest in fluidization. Thus, in order to pursue the theoretical calculation he is forced to make assumptions, namely that the diffusivity defined in [9] is $O(1)$, as suggested by sedimentation experiments, and that momentum transfer by fluctuations in particle concentration is negligible. Neither of these assumptions can be justified *a priori*, in spite of the arguments he gives. Our results can be interpreted as implying that the opposite is true; our experiments were done in a range of particle Re for which the *scaling* for the gradient diffusivity in [9] is expected to be valid. Thus, if the elasticity due to dispersion dominated, the inferred values of Q in these scalings would be expected to be constant with particle Re over some range. The results in figures 8(a, b) therefore may be interpreted as implying that the small constant term in the deduced expression is due to a very small gradient diffusivity at these high volume concentrations, and that the origin of the elasticity is inertial in nature. Moreover, the dependence of Q on R, i.e. the particle density is what matters, shows that the physical mechanism is most likely due to the Reynolds stress due to particle velocity fluctuations.

Acknowledgements—Much of this work is based upon the Ph.D. research of J. Ham, supported by a grant from the NSF, Multiphase and Particulate Processing Program. S. Thomas did the early exploratory experiments that indicated the existence of stable fluidization under the sponsorship of the Proctor & Gamble Undergraduate Research Program. E. Guazzelli was supported by a CNRS–NSF Exchange Program, Sept. 1987–Sept. 1988. M.-C. Anselmet did the experiments with different fluids during a short stay sponsored by a travel grant from the University of Provence. The final series of experiments was made possible by a travel grant to E. Guazzelli from the French Foreign Minister. We thank Pierre Magnico of ESPCI, Paris, for help in preparing particles. The glass beads were provided by Cataphote Corp., and the acrylic beads by duPont and Orkem Norsolor. We also benefitted from helpful discussions with Professor G. K. Batchelor, made possible through a NATO Travel Grant.

REFERENCES

ANDERSON, T. B. & JACKSON, R. 1967 A fluid mechanical description of fluidized beds: equations of motion. *Ind. Engng Chem. Fundam.* **6,** 527–539.

ANDERSON, T. B. & JACKSON, R. 1968 A fluid mechanical description of fluidized beds: stability of the state of uniform fluidization. *Ind. Engng Chem. Fundam.* **7,** 12–21.

ANDERSON, T. B. & JACKSON, R. 1969 A fluid mechanical description of fluidized beds: comparison of theory and experiment. *Ind. Engng Chem. Fundam.* **8,** 137–144.

BATCHELOR, G. K. 1988 A new theory of the instability of a uniform fluidized bed. *J. Fluid Mech.* **193,** 75–110.

DAVIDSON, J. F., CLIFT, R. & HARRISON, D. (Eds) 1985 *Fluidization*, 2nd edn. Academic Press, London.

DAVIS, R. H. & HASSEN, M. A. 1988 Spreading of the interface at the top of a slightly polydisperse sedimenting suspension. *J. Fluid Mech.* **196,** 107–134.

DIDWANIA, A. K. & HOMSY, G. M. 1981 Flow regimes and flow transitions in liquid fluidized beds. *Int. J. Multiphase Flow* **7,** 563–580.

DREW, D. & SEGEL, L. A. 1971a Averaged equations for two-phase flows. *Stud. appl. Math.* **50,** 205–231.

DREW, D. A. & SEGEL, L. A. 1971b Analysis of fluidized beds and foams using averaged equations. *Stud. appl. Math.* **50,** 233–257.

EL-KAISSY, M. M. & HOMSY, G. M. 1976 Instability waves and the origin of bubbles in fluidized beds—I. Experiments. *Int. J. Multiphase Flow* **2,** 379–395.

FOSCOLO, P. U. & GIBILARO, L. G. 1984 A fully predictive criterion for the transition between particulate and aggregative fluidization. *Chem. Engng Sci.* **39,** 1667–1675.

HAM, J. M. 1988 Ph.D. Thesis, Dept of Chemical Engineering, Stanford Univ., Calif.

HAM, J. M. & HOMSY, G. M., 1988 Hindered settling and hydrodynamic dispersion in quiescent sedimenting suspensions. *Int. J. Multiphase Flow* **14,** 533–546.

HOMSY, G. M. 1983 A survey of some results in the mathematical theory of fluidization. In *Theory of Dispersed Multiphase Flow* (Edited by MEYER, R. E.), pp. 57–71. Academic Press, New York.

HOMSY, G. M., EL-KAISSY M. M., & DIDWANIA, A. K. 1980 Instability waves and the origin of bubbles in fluidized beds—II. Comparison with theory. *Int. J. Multiphase Flow* **6,** 305–318.

JACKSON, R. 1985 In *Fluidization*, 2nd edn (Edited by DAVIDSON, J. F., CLIFT, R. & HARRISON, D.), pp. 47–72. Academic Press, London.

LIU, J. T. C. 1982 Note on a wave-hierarchy interpretation of fluidized bed instabilities. *Proc. R. Soc. Lond.* **A380,** 229–239.

RICHARDSON, J. F. & ZAKI, W. N. 1954 Sedimentation and fluidization: Part I. *Trans. Instn chem. Engrs* **32,** 35–53.

WHITAM, G. B. 1974 *Linear and Nonlinear Waves*. Wiley, New York.

APPENDIX

We exhibit the working formula used to reduce the measured stability limits to values of the effective diffusivity. We begin with [6] of the main text:

$$Z = \frac{K_0}{u_0^2} + \frac{\gamma_0(1-R)\hat{D}_0}{\mathrm{Fr}_0}. \qquad [A.1]$$

In this formula

$$K_0 = -\left[\frac{\mathrm{d}}{\mathrm{d}\epsilon}\left((1-\epsilon_0)Hu_0^2\right)\right]_0, \qquad [A.2]$$

where $H(\epsilon)u_0^2$ is the proposed form for $\langle V^2\rangle$ in a homogeneous bed,

$$R = \frac{\rho_\mathrm{f}}{\rho_\mathrm{s}} \qquad [A.3]$$

is the ratio of the density,

$$\gamma = \frac{V}{F_\mathrm{h}}\left[\frac{\partial F_\mathrm{h}}{\partial V}\right]_{\phi\ \mathrm{const}} \qquad [A.4]$$

is the drag slope parameter,

$$\mathrm{Fr}_0 = \frac{u_0^2}{gd} \qquad [A.5]$$

is the Froude number and

$$\hat{D}_0 = \frac{D}{du_0}, \qquad [A.6]$$

where D is the hydrodynamic (gradient) diffusivity of the particles. Using these definitions, we can rewrite [11] as

$$Q > \frac{\mathrm{Fr}_0(1-\epsilon_0)^2 n^2}{(1-R)\gamma_0 \epsilon_0^2}\left[(1-R)+\frac{3R(n-1)}{2n\epsilon_0}\right]. \qquad [A.7]$$

Here n is the Richardson–Zaki exponent (Richardson & Zaki 1954) and A, B and C have been replaced by the forms proposed by Batchelor, where, in his notation,

$$\theta = Rc(\epsilon), \qquad [A.8]$$

$$\zeta = -R(1-\epsilon)\frac{\mathrm{d}c}{\mathrm{d}\epsilon} \qquad [A.9]$$

and

$$c(\epsilon) = \frac{3-2\epsilon}{2\epsilon}. \qquad [A.10]$$

Values for γ can be obtained from the definition of γ given after [B.4] in Batchelor (1988) and the formula F_h taken from Batchelor (1988) and presented here as [A.12]. The resulting formula for γ is given in [A.13], which shows the dependence of γ on the drag coefficient C_D. In general, C_D will depend upon ϵ, R, the particle configuration and the particle Re:

$$\mathrm{Re} \equiv \frac{v d \rho_f}{\mu}, \qquad [A.11]$$

$$F_h = -\tfrac{1}{2}\pi a^2 \rho_f v^2 C_D \qquad [A.12]$$

and

$$\gamma = 2 + \frac{v}{C_D}\frac{\partial C_D}{\partial v}. \qquad [A.13]$$

For the purposes of this study, we will follow Batchelor, who considers γ to be relatively insensitive to ϵ and therefore takes $C_D = C_{D0}$, where C_{D0} is the drag coefficient for an isolated rigid sphere. In particular, we will use the correlation for C_{D0} from Foscolo & Gibilaro (1984), which is used by Batchelor for $0 < \mathrm{Re} < 2000$, i.e.

$$C_{D0} = \left(0.63 + \frac{4.90}{\sqrt{\mathrm{Re}}}\right)^2. \qquad [A.14]$$

The working formula for γ is given in [A.15], from which it can be seen that the value for γ has a relatively small influence on Q, varying from 1 when $\mathrm{Re} \ll 1$ to 2 when $\mathrm{Re} \gg 1$:

$$\gamma = 1 + \frac{0.63\sqrt{\mathrm{Re}}}{4.90 + 0.63\sqrt{\mathrm{Re}}}. \qquad [A.15]$$

Equation [A.7] can be used to determine the magnitude of Q required to stabilize a given bed at minimum fluidization or to determine the actual value of $\hat{D}_0$ for a given system.